A Novel Method for Modeling Coupling Between Several Microstrip Lines in MIC's and MMIC's

Daniel G. Swanson, Jr., *Member, IEEE*

Abstract—**This paper presents a novel technique for modeling the adjacent and nonadjacent couplings between several microstrip lines. The technique assumes that the primary transmission paths in the circuit can be modeled with conventional single or coupled microstrip models. A new four-port model is then superimposed on the existing circuit for each adjacent or nonadjacent coupling that is present. The new model uses analytical equations for microstrip coupled lines and is, therefore, fast and easy to compute.**

I. Introduction

MULTIPLE microstrip lines running in parallel are found quite often in MIC and MMIC circuit layouts. Multiple coupled lines are used by design in many circuits including interdigital and hairpin filters, meander lines, and spiral inductors. In these cases, the couplings between multiple lines are an important part of the desired response and must be modeled accurately. Undesired couplings can occur when circuits are tightly packed into a small physical space, such as the multiple drain and gate lines in a matrix amplifier MMIC chip (Fig. 1). In MIC's and MMIC's, these undesired couplings can lead to unexpected deleterious results and even to spurious oscillations.

Some very sophisticated numerical techniques exist for analyzing multiple microstrip coupled lines. Some examples of these techniques are the spectral-domain method [1], the method of moments [2], and the finite element method [3]. While the accuracy of these methods is high, lengthy computation times have made their implementation in interactive microwave CAD programs impractical. Only one commercial CAD package [4] has overcome this time barrier by employing interpolation in a precomputed, multidimensional data base.

The technique presented here utilizes a new four-port model called the generalized coupling model (GCM). The new model allows weakly coupled adjacent and nonadjacent lines to be modeled without modifying the underlying circuit structure. This method assumes that the primary transmission paths in the circuit can be modeled with conventional single or coupled microstrip models.

Manuscript received September 5, 1990; revised January 29, 1991.

The author is with the Watkins-Johnson Company, 3333 Hillview Ave., Palo Alto, CA 94304-1204.

IEEE Log Number 9144291.

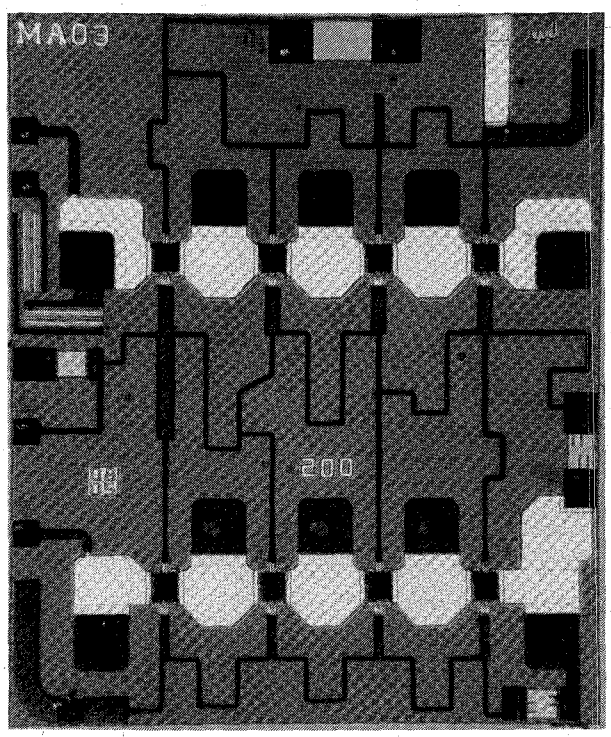

Fig. 1. GaAs monolithic matrix amplifier.

The GCM is then superimposed on the existing circuit for each adjacent or nonadjacent coupling that is present. The parameters of the GCM can be computed very quickly using analytical formulas for microstrip coupled lines [5]. The technique presented here, while it is an approximation, can be applied to the circuit model at any time. Initial design and optimization can be performed without considering coupling effects and the coupling model can be added in the later stages of the design cycle. At worst, a few new nodes may have to be created in the circuit description to accommodate the GCM.

II. Theory

The generalized coupling model was developed by examining the Y matrix for the microstrip coupled line pair shown in Fig. 2. There are four unique terms in the

0018-9480/91/0600-0917$01.00 ©1991 IEEE

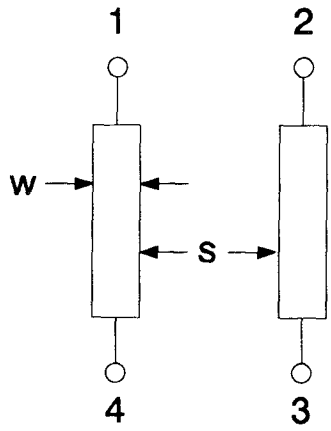

Fig. 2. Microstrip coupled line pair.

four-port Y matrix for lossless coupled microstrip lines [6]. The four terms are labeled $Y1$ through $Y4$ to emphasize the symmetry in the Y matrix:

$$Y1 = -j\frac{1}{2}[Y_{0e}\cot\theta_e + Y_{0o}\cot\theta_o] \quad (1)$$

$$Y2 = -j\frac{1}{2}[Y_{0e}\cot\theta_e - Y_{0o}\cot\theta_o] \quad (2)$$

$$Y3 = +j\frac{1}{2}[Y_{0e}\csc\theta_e - Y_{0o}\csc\theta_o] \quad (3)$$

$$Y4 = +j\frac{1}{2}[Y_{0e}\csc\theta_e + Y_{0o}\csc\theta_o]. \quad (4)$$

In matrix notation;

$$Y = \begin{vmatrix} Y1 & Y2 & Y3 & Y4 \\ Y2 & Y1 & Y4 & Y3 \\ Y3 & Y4 & Y1 & Y2 \\ Y4 & Y3 & Y2 & Y1 \end{vmatrix}. \quad (5)$$

In the limit as the spacing, s, between the lines becomes large, the coupled line pair behaves as two independent single lines. Four terms in the Y matrix can be identified with the single line connected between nodes one and four:

$$Y = \begin{vmatrix} Y1 & 0 & 0 & Y4 \\ 0 & 0 & 0 & 0 \\ 0 & 0 & 0 & 0 \\ Y4 & 0 & 0 & Y1 \end{vmatrix}. \quad (6)$$

These four terms describe the self-admittance and the transfer admittance of the single line. In a similar fashion, four different terms in the Y matrix can be identified with the single line connected between nodes two and three:

$$Y = \begin{vmatrix} 0 & 0 & 0 & 0 \\ 0 & Y1 & Y4 & 0 \\ 0 & Y4 & Y1 & 0 \\ 0 & 0 & 0 & 0 \end{vmatrix}. \quad (7)$$

Eight of the 16 terms in the Y matrix for the coupled line pair have now been identified with the individual lines. The remaining eight terms on the edges of the matrix must describe the coupling between the two lines:

$$Y = \begin{vmatrix} 0 & Y2 & Y3 & 0 \\ Y2 & 0 & 0 & Y3 \\ Y3 & 0 & 0 & Y2 \\ 0 & Y3 & Y2 & 0 \end{vmatrix}. \quad (8)$$

Only these eight terms on the edges of the Y matrix are used in the generalized coupling model. Because only the "coupling" terms are used, the model can be applied many times without significantly modifying the self-admittance or the transfer-admittance terms in the underlying circuit. For weakly coupled microstrips, the Y-matrix terms computed for an isolated pair of coupled microstrips are sufficiently accurate.

A simple meander-line example will demonstrate how the nodal Y matrix is modified to account for coupling. The meander-line circuit and node numbering scheme are shown in Fig. 3(a). It is assumed for this example that the line widths are equal and the spaces between lines are equal. The circuit is first modeled with single microstrip lines. The two unique Y-matrix entries for a lossless microstrip single line are

$$Y_{S1} = -jY_0\cot(\theta) \quad (9)$$

and

$$Y_{S2} = +jY_0\csc(\theta). \quad (10)$$

Y_{S1} and Y_{S2} are computed using the width and length of the three longer microstrip lines. The characteristic admittance and theta are computed using any convienient set of analytical equations for single microstrip lines. Similarly, Y'_{S1} and Y'_{S2} are computed with (9) and (10) using the width and length of the two shorter microstrip

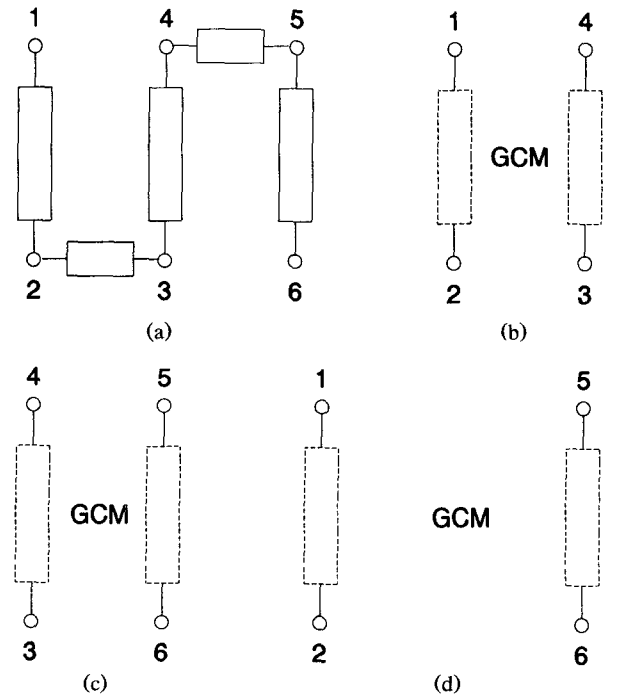

Fig. 3. (a) Microstrip meander-line. (b) GCM superimposed at nodes one, four, three and two. (c) GCM superimposed at nodes four, five, six and three. (d) GCM superimposed at nodes one, five, six and two.

lines. The nodal Y martix for the circuit modeled with single microstrip lines is

$$Y = \begin{vmatrix} Y_{S1} & Y_{S2} & 0 & 0 & 0 & 0 \\ Y_{S2} & Y_{S1}+Y'_{S1} & Y'_{S2} & 0 & 0 & 0 \\ 0 & Y'_{S2} & Y_{S1}+Y'_{S1} & Y_{S2} & 0 & 0 \\ 0 & 0 & Y_{S2} & Y_{S1}+Y'_{S1} & Y'_{S2} & 0 \\ 0 & 0 & 0 & Y'_{S2} & Y_{S1}+Y'_{S1} & Y_{S2} \\ 0 & 0 & 0 & 0 & Y_{S2} & Y_{S1} \end{vmatrix}. \tag{11}$$

At this point the circuit could be analyzed from nodes one to six without coupling taken into account. Next, the coupling from the first strip to the second strip is added by superimposing the GCM at nodes one, four, three, and two as shown in Fig. 3(b). Y_{C2} and Y_{C3} are computed with (2) and (3) using the width, length, and spacing of the first and second coupled lines as if they were an isolated coupled line pair. The even and odd mode admittances and phase velocities are computed using [5]. The new nodal Y matrix is

$$Y = \begin{vmatrix} Y_{S1} & Y_{S2} & Y_{C3} & Y_{C2} & 0 & 0 \\ Y_{S2} & Y_{S1}+Y'_{S1} & Y'_{S2}+Y_{C2} & Y_{C3} & 0 & 0 \\ Y_{C3} & Y'_{S2}+Y_{C2} & Y_{S1}+Y'_{S1} & Y_{S2} & 0 & 0 \\ Y_{C2} & Y_{C3} & Y_{S2} & Y_{S1}+Y'_{S1} & Y'_{S2} & 0 \\ 0 & 0 & 0 & Y'_{S2} & Y_{S1}+Y'_{S1} & Y_{S2} \\ 0 & 0 & 0 & 0 & Y_{S2} & Y_{S1} \end{vmatrix}. \tag{12}$$

Next, the coupling from the second strip to the third strip is added by superimposing the GCM at nodes four, five, six, and three as shown in Fig. 3(c). Y_{C2} and Y_{C3} are computed with (2) and (3) using the width, length, and spacing of the second and third coupled lines as if they were an isolated coupled line pair. Owing to the symmetry of this example circuit, the Y_{C2} and Y_{C3} computed at this step are the same as the Y_{C2} and Y_{C3} computed for the previous step. The nodal Y matrix at this step is

$$Y = \begin{vmatrix} Y_{S1} & Y_{S2} & Y_{C3} & Y_{C2} & 0 & 0 \\ Y_{S2} & Y_{S1}+Y'_{S1} & Y'_{S2}+Y_{C2} & Y_{C3} & 0 & 0 \\ Y_{C3} & Y'_{S2}+Y_{C2} & Y_{S1}+Y'_{S1} & Y_{S2} & Y_{C3} & Y_{C2} \\ Y_{C2} & Y_{C3} & Y_{S2} & Y_{S1}+Y'_{S1} & Y'_{S2}+Y_{C2} & Y_{C3} \\ 0 & 0 & Y_{C3} & Y'_{S2}+Y_{C2} & Y_{S1}+Y'_{S1} & Y_{S2} \\ 0 & 0 & Y_{C2} & Y_{C3} & Y_{S2} & Y_{S1} \end{vmatrix}. \tag{13}$$

Finally, the coupling from the first to the third line is added to they Y matrix by superimposing the GCM at nodes one, five, six, and two as shown in Fig. 3(d). Y'_{C2} and Y'_{C3} are computed with (2) and (3) using the width, length, and spacing of the first and third coupled lines as if they were an isolated coupled line pair. The final nodal Y matrix is

$$Y = \begin{vmatrix} Y_{S1} & Y_{S2} & Y_{C3} & Y_{C2} & Y'_{C2} & Y'_{C3} \\ Y_{S2} & Y_{S1}+Y'_{S1} & Y'_{S2}+Y_{C2} & Y_{C3} & Y'_{C3} & Y'_{C2} \\ Y_{C3} & Y'_{S2}+Y_{C2} & Y_{S1}+Y'_{S1} & Y_{S2} & Y_{C3} & Y_{C2} \\ Y_{C2} & Y_{C3} & Y_{S2} & Y_{S1}+Y'_{S1} & Y'_{S2}+Y_{C2} & Y_{C3} \\ Y'_{C2} & Y'_{C3} & Y_{C3} & Y'_{S2}+Y_{C2} & Y_{S1}+Y'_{S1} & Y_{S2} \\ Y'_{C3} & Y'_{C2} & Y_{C2} & Y_{C3} & Y_{S2} & Y_{S1} \end{vmatrix}. \tag{14}$$

The circuit can now be analyzed from port one to port six with adjacent and non adjacent couplings taken into account. The final example in this paper will present measured and computed data for a similar meander-line circuit.

It is helpful to put a numerical measure on the accuracy of this technique. One way is to compare the accuracy of predicted coupling from port one to port two for an ideal microstrip four-port and a pair of single microstrip lines with the new coupling model superimposed

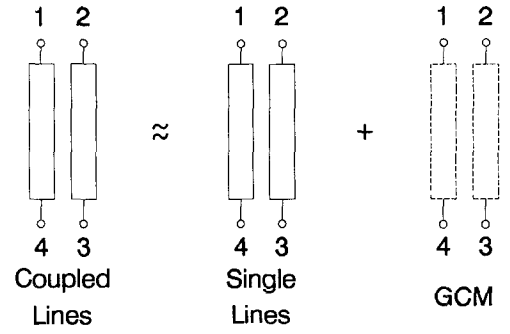

Fig. 4. Comparison of conventional microstrip coupled line model with two single microstrip lines with GCM superimposed.

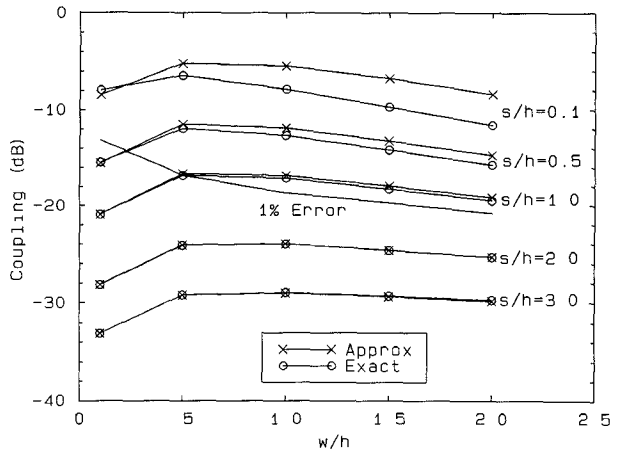

Fig. 5. Results of the comparison outlined in Fig. 4 for coupled lines 95 mil long on 15-mil-thick alumina, $\epsilon_r = 9.8$. The analysis frequency is 12 GHz.

(see Fig. 4). In matrix form this comparison is

$$\begin{vmatrix} Y1 & Y2 & Y3 & Y4 \\ Y2 & Y1 & Y4 & Y3 \\ Y3 & Y4 & Y1 & Y2 \\ Y4 & Y3 & Y2 & Y1 \end{vmatrix} \approx \begin{vmatrix} Y_{S1} & 0 & 0 & Y_{S2} \\ 0 & Y_{S1} & Y_{S2} & 0 \\ 0 & Y_{S2} & Y_{S1} & 0 \\ Y_{S2} & 0 & 0 & Y_{S1} \end{vmatrix} + \begin{vmatrix} 0 & Y2 & Y3 & 0 \\ Y2 & 0 & 0 & Y3 \\ Y3 & 0 & 0 & Y2 \\ 0 & Y3 & Y2 & 0 \end{vmatrix}. \quad (15)$$

The results of this analysis for a pair of coupled lines on alumina are shown in Fig. 5. The microstrip lines were 95 mil long on a 15-mil-thick alumina substrate. The analysis was performed at 12 GHz where the coupled length is approximately one quarter wavelength. For spacing to height ratios greater than 1, the difference in predicted coupling between the two methods is less than 1%.

III. Applications

This new four-port coupling model has been implemented as a user-defined element in TOUCHSTONE SR. [7] and SUPER-COMPACT MAINFRAME [8]. The model accepts physical dimensions for coupled line pairs and calculates Y parameters using [5] and [6].

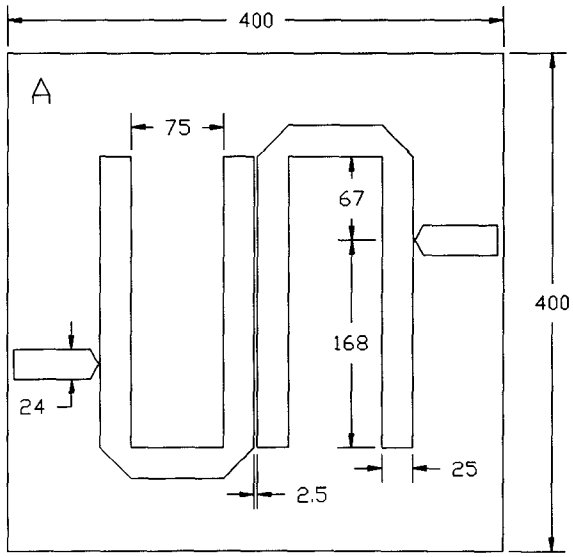

Fig. 6. Detail of microstrip hairpin filter A, alumina substrate, $h = 25$ mil, $\epsilon_r = 9.8$. Dimensions computed with parasitic couplings taken into account. All dimensions are mils.

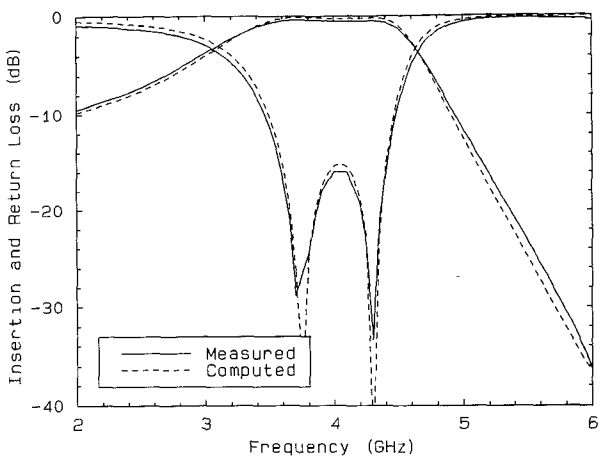

Fig. 7. Measured versus computed response for microstrip hairpin filter A when adjacent and nonadjacent couplings are taken into account using the GCM.

A microstrip hairpin filter is the first example of how this technique can be applied. Hairpin filter A (Fig. 6) was designed for a 20% bandwidth at 4 GHz using the generalized coupling model to predict couplings across the resonator arms and nonadjacent couplings between resonators. The measured and computed responses shown in Fig. 7 are in close agreement for hairpin filter A. Hairpin filter B (Fig. 8) was also designed for a 20% bandwidth at 4 GHz but parasitic couplings were ignored at the design stage. Fig. 9 shows the measured versus computed performance for hairpin filter B. The error between computed and measured bandwidthes at the lower band edge is 148 MHz, or 18.5% of the desired 800 MHz bandwidth.

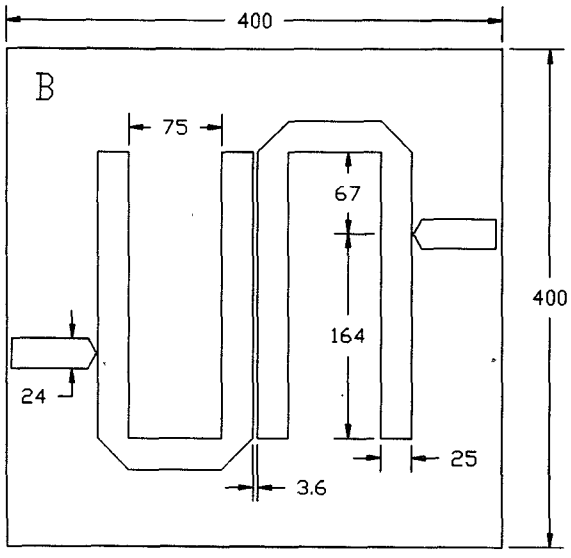

Fig. 8. Detail of microstrip hairpin filter B, alumina substrate, $h = 25$ mil, $\epsilon_r = 9.8$. Dimensions computed with parasitic couplings ignored. All dimensions are mils.

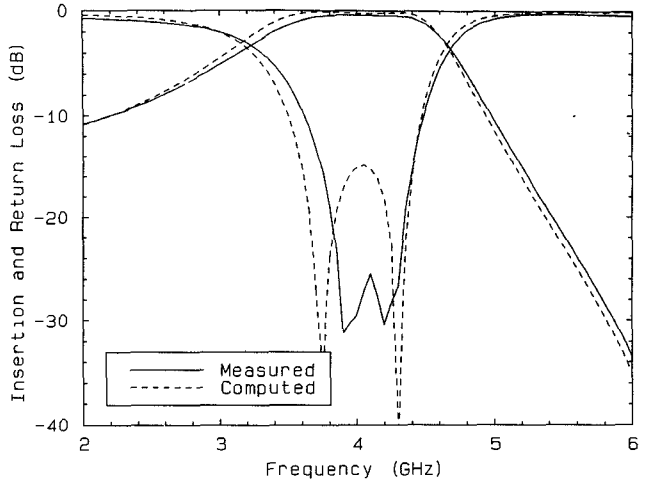

Fig. 9. Measured versus computed response for microstrip hairpin filter B when adjacent and nonadjacent couplings are ignored.

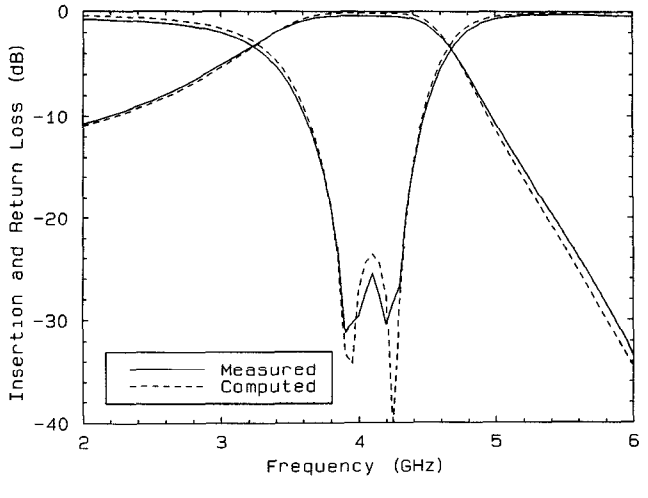

Fig. 10. Measured versus computed response for microstrip hairpin filter B when the GCM model is applied to the as-built dimensions.

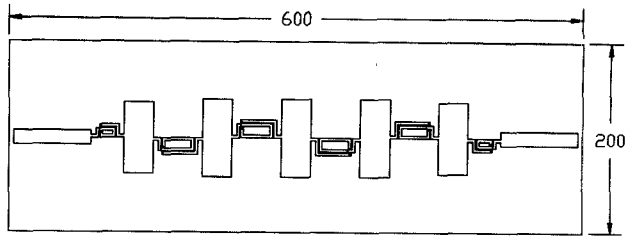

Fig. 11. Microstrip low-pass filter using thin-film spiral inductors, alumina substrate, $h = 15$ mil, $\epsilon_r = 9.8$. All dimensions are mils.

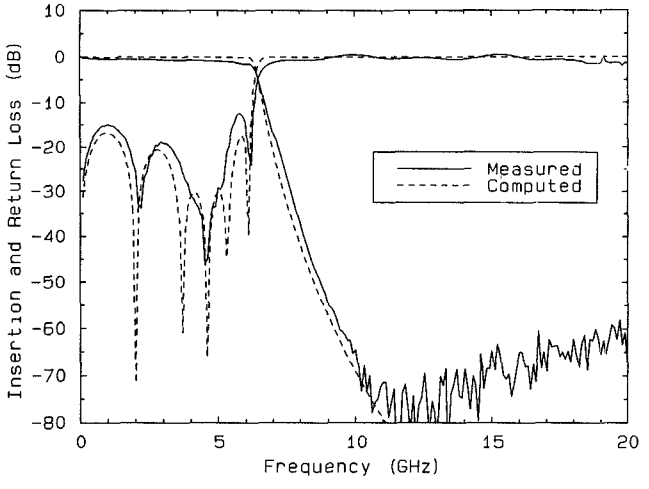

Fig. 12. Measured and computed data for the microstrip low-pass filter when mutual couplings in the spiral inductors are modeled using the GCM.

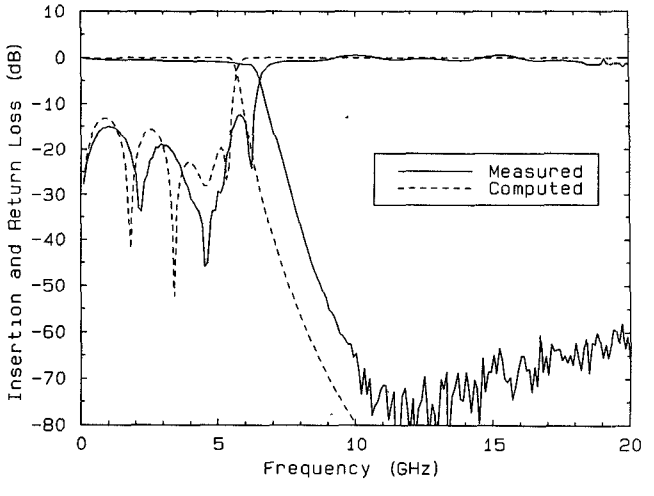

Fig. 13. Measured and computed data for the microstrip low-pass filter when mutual couplings in the spiral inductors are ignored.

To conclude the analysis of these filters, parasitic coupling was added to the computer model for hairpin filter B. With the GCM applied to the as-built dimensions, the measured and computed responses shown in Fig. 10 are now in close agreement. Tuning was not required to achieve the results presented here. It is also interesting to note that the parasitic couplings in the hairpin filter are destructive. That is, to achieve the proper bandwidth, the

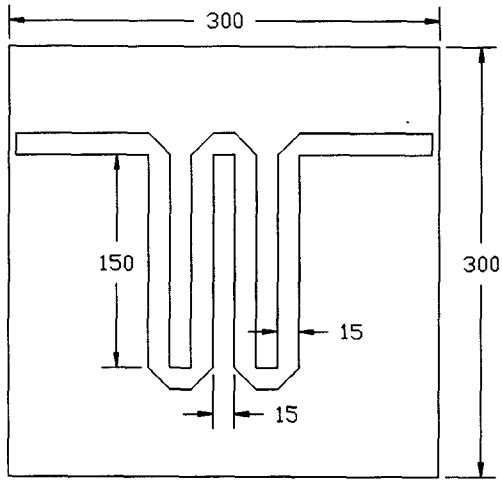

Fig. 14. Detail of microstrip meander line, alumina substrate, $h = 15$ mil, $\epsilon_r = 9.8$. All dimensions are mils.

gap between resonators in filter A is smaller than the gap in filter B.

The second example is a 6.2 GHz microstrip low-pass filter using printed spiral inductors [9], as shown in Fig. 11. The fundamental computer model for the spiral inductor uses coupled and single microstrip lines [10]. The generalized coupling model is applied six times to each spiral to model the mutual couplings across the spiral. The measured-versus-computed data for this filter are shown in Fig. 12. If the mutual couplings across each spiral are not modeled, the computer prediction is much less accurate, as shown in Fig. 13. When mutual couplings are ignored the error between computed and measured filter cutoff frequency is 750 MHz.

The final example is a microstrip meander line, as shown in Fig. 14. Without modeling coupling between the lines, the computer predicts no loss other than ohmic losses for this circuit. In reality, there is significant loss as the coupled length approaches half a wavelength. The GCM was applied to this circuit eight times to model the coupling between strips. The measured-versus-computed insertion loss, return loss, and insertion phase responses are shown in parts (a)–(c) of Fig. 15.

Because all the modes present in this multiconductor circuit cannot be fully described by an approximate method [11], the computed responses for the meander line lose accuracy as the coupled length passes through one half wavelength. However, the analysis time for this circuit using the generalized coupling model was approximately 5 s, and at frequencies below the half-wavelength frequency the modeling accuracy is quite good. When the same circuit was analyzed using a spectral-domain multistrip model [8] no accuracy was lost at the half-wavelength frequency, but the analysis time was approximately 5 min.

IV. Conclusion

A new generalized coupling model has been developed which allows weak coupling between adjacent and nonadjacent coupled microstrip lines to be accurately modeled.

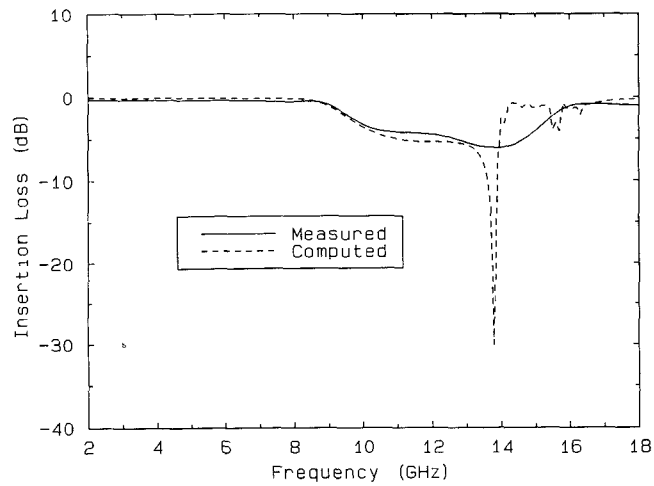

(a)

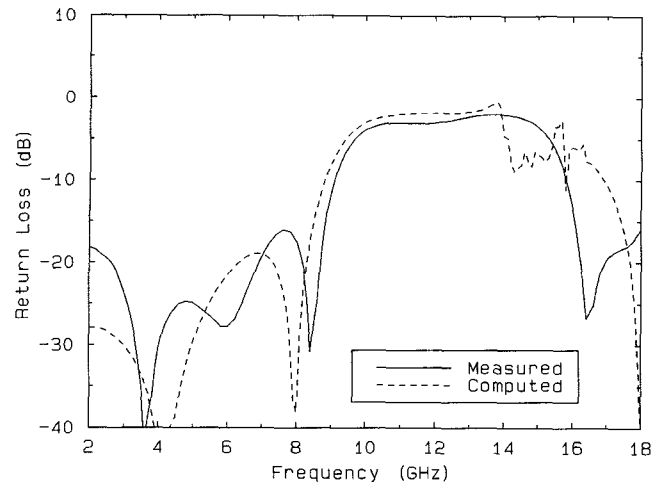

(b)

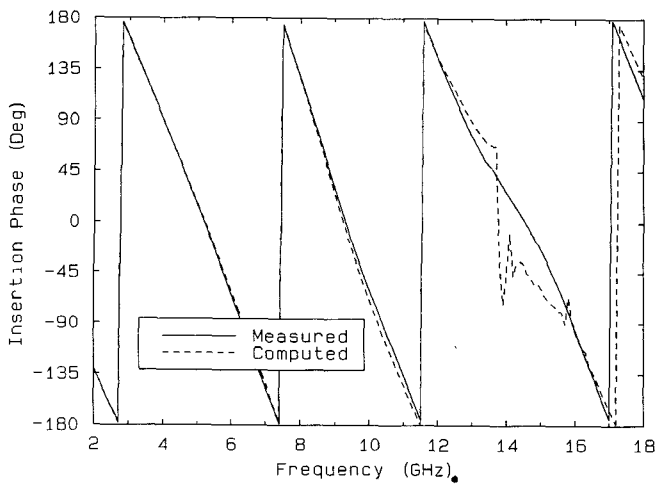

(c)

Fig. 15. Measured and computed (a) insertion loss, (b) return loss, and (c) insertion phase for the microstrip meander line when adjacent and nonadjacent couplings are modeled using the GCM.

The model uses analytical equations for coupled microstrip lines and is, therefore, fast and easy to compute. It is assumed that the weak couplings modeled by the GCM have a negligible influence on ohmic losses; thus the GCM is a lossless model.

Best results using the generalized coupling model are obtained when any strong couplings in the circuit can be described using isolated coupled line pairs while only weak couplings are modeled using the GCM. The hairpin filter and low-pass filter examples demonstrate the utility of the GCM under these conditions. The microstrip meander-line example was designed to test the limits of the GCM for tight coupling and long coupled lengths. Accuracy is indeed lost for coupled lengths in the vicinity of one half wavelength but the computation time for this technique is quite low compared with other methods.

References

[1] R. H. Jansen, "Unified user-oriented computation of shielded, covered and open planar microwave and millimeter-wave transmission-line characteristics," *IEE J. Microwaves, Opt. Acoust.*, vol. 3, pp. 14–22, Jan. 1979.

[2] Cao Wei, R. F. Harrington, J. R. Mautz, and T. K. Sarkar, "Multiconductor transmission lines in multilayered dielectric media," *IEEE Trans. Microwave Theory Tech.*, vol. MTT-32, pp. 439–450, Apr. 1984.

[3] P. Daly, "Hybrid-mode analysis of microstrip by finite element method," *IEEE Trans. Microwave Theory Tech.*, vol. MTT-19, pp. 19–25, Jan. 1971.

[4] LINMIC+, Jansen Microwave, Ratingen, West Germany.

[5] M. Kirschning and R. H. Jansen, "Accurate wide-range design equations for the frequency dependent characteristics of parallel coupled microstrip lines," *IEEE Trans. Microwave Theory Tech.*, vol. MTT-32, pp. 83–90, Jan. 1984.

[6] G. Zysman and A. Johnson, "Coupled transmission line networks in an inhomogeneous dielectric medium," *IEEE Trans. Microwave Theory Tech.*, vol. MTT-17, pp. 753–759, Oct. 1969.

[7] TOUCHSTONE SR., EEsof Inc., Westlake Village, CA.

[8] SUPER-COMPACT, Compact Software Inc., Paterson, NJ.

[9] D. Swanson, "Thin-film lumped-element microwave filters," in *1989 IEEE MTT-S Int. Microwave Symp. Dig.* (Long Beach), pp. 671–674.

[10] D. Cahana, "A new transmission line approach for designing spiral microstrip inductors for microwave integrated circuits," in *1983 IEEE MTT-S Int. Microwave Symp. Dig.* (Boston), pp. 245–247.

[11] A. R. Dalby, "Interdigital microstrip circuit parameters using empirical formulas and simplified model," *IEEE Trans. Microwave Theory Tech.*, vol. MTT-27, pp. 744–752, Aug. 1979.

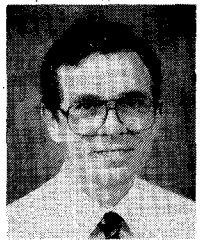

Daniel G. Swanson, Jr. (S'74–M'78) received the B.S.E.E degree from the University of Illinois in 1976 and the M.S.E.E. degree from the University of Michigan in 1978.

In 1978 he joined Narda Microwave, where he developed a 6–18 GHz low-noise amplifier, an 8–10 GHz low-noise amplifier, and a de-embedding system for *S*-parameter device characterization. In 1980 he was with the Wiltron Company designing YIG tuned oscillators for use in microwave sweepers. He also developed a broad-band load-pull system for optimization of output power. In 1983, Mr. Swanson joined a startup company, Iridian Microwave, where he was responsible for the dielectric resonator oscillator product line. In 1984 he joined Avantek Inc., where he developed thin-film microwave filters, software for filter design, and a low-frequency broad-band GaAs MMIC amplifier. In 1989, he joined the Watkins-Johnson Company where he is Staff Scientist. His current work encompasses thin-film filters, miniature cavity filters, and voltage-controlled oscillators.

Mr. Swanson served as an officer in the Santa Clara Valley Chapter of the Microwave Theory and Techniques Society from 1985 to 1989. He is serving as MTT-S AdCom Secretary for 1991. Mr. Swanson is a member of Eta Kappa Nu.